BIOCHEMISTRY
including biophysical chemistry & molecular biology

Article

pubs.acs.org/biochemistry

The Sigma Enigma: *In Vitro/in Silico* Site-Directed Mutagenesis Studies Unveil σ_1 Receptor Ligand Binding

S. Brune,[†] D. Schepmann,[†] K.-H. Klempnauer,[‡] D. Marson,[§] V. Dal Col,[§] E. Laurini,[§] M. Fermeglia,[§] B. Wünsch,*[,†] and S. Pricl*[,§,∥]

[†]Institut für Pharmazeutische und Medizinische Chemie, Westfälische Wilhelms-Universität Münster, Corrensstraße 48, D-48149 Münster, Germany

[‡]Institut für Biochemie, Westfälischen Wilhelms-Universität Münster, Wilhelm-Klemm-Straße 2, D-48149 Münster, Germany

[§]Molecular Simulation Engineering (MOSE) Laboratory, Department of Engineering and Architecture (DEA), University of Trieste, Via Valerio 10, 34127 Trieste, Italy

[∥]National Interuniversity Consortium for Material Science and Technology (INSTM), Research Unit MOSE-DEA, University of Trieste, Trieste, Italy

Supporting Information

ABSTRACT: The σ_1 receptor is an integral membrane protein that shares no homology with other receptor systems, has no unequivocally identified natural ligands, but appears to play critical roles in a wide variety of cell functions. While the number of reports of the possible functions of the σ_1 receptor is increasing, almost no information about the three-dimensional structure of the receptor and/or possible modes of interaction of the σ_1 protein with its ligands have been described. Here we performed an *in vitro/in silico* investigation to analyze the molecular interactions of the σ_1 receptor with its prototypical agonist (+)-pentazocine. Accordingly, 23 mutant σ_1 isoforms were generated, and their interactions with (+)-pentazocine were determined experimentally. All direct and/or indirect effects exerted by the mutant residues on the receptor−agonist interactions were reproduced and rationalized *in silico*, thus shining new light on the three-dimensional structure of the σ_1 receptor and its ligand binding site.

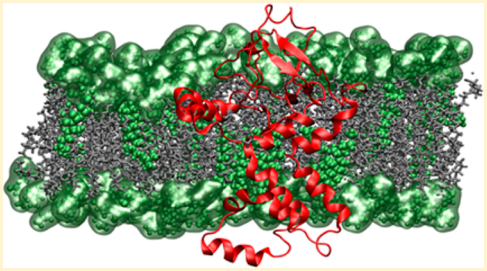

The σ_1 receptor was originally identified and classified as an opioid and phencyclidine (PCP) receptor.[1] The term opioid refers to a receptor's ability to bind naloxone or naltrexone; because the σ_1 receptor binds both these ligands with very low affinity,[2] it was subsequently reclassified as a non-opioid receptor. Additionally, the σ_1 receptor was determined not to be the site of high-affinity PCP binding, which was identified as the *N*-methyl-D-aspartate (NMDA) receptor.[3] The identification of some selective σ_1 ligands coupled with the discovery of σ_1 function modulation by endogenous compounds such as progesterone, D-*erythro*-sphingosine, *N*,*N*-dimethyltryptamine, and other endogenous lipids[4,5] finally allowed the conclusion that the σ_1 receptor represents a distinct binding site in the central nervous systems (CNS) and peripheral organs.

The σ_1 receptor, cloned for the first time in 1996,[6,7] is an integral membrane protein of 223 amino acids, predominantly found in the endoplasmic reticulum (ER). All mammalian σ_1 receptors are 90% identical and 95% similar in terms of amino acid sequence across species. The most recent evidence indicates that the σ_1 receptor is a novel ER chaperone, which is involved in a number of cellular functions, including inositol 1,4,5-triphosphate (IP3) receptor-mediated Ca^{2+} signaling, ion channel firing, protein kinase location and/or activation, cellular redox, neurotransmitter release, inflammation, cellular differentiation, neuronal survival, and synaptogenesis.[8] An intriguing aspect of σ_1 receptors is that they can bind, with moderate to high affinity, a wide spectrum of compounds of very different structural classes and diverse therapeutic and pharmacological applications. For instance, σ_1 antagonists can be used for the treatment of psychosis, as they do not lead to the extrapyramidal motoric side effects of typical D_2 receptor antagonists. Also, σ_1 ligands represent a new paradigm for the treatment of neuropathic pain, depression, cocaine abuse, and epilepsy. Neuroprotective and antiamnesic properties of some σ_1 ligands have been tested in the treatment of diseases associated with the loss of cognitive function, e.g., Alzheimer's disease and Parkinson's disease.[8−11] Furthermore, σ_1 ligands may be used in cancer therapy and diagnosis, because σ_1 receptors are strongly expressed in tumor cells.[12,13]

Several synthetic molecules belonging to different structural classes were thus found to bind to the σ_1 receptor. (+)-Pentazocine (PTZ) represents a very potent and highly selective σ_1 agonist, which is used as a "gold standard" in σ_1 ligand binding studies.[14] Prototypical σ_1 antagonists with high receptor affinity are NE-100[15] and the neuroleptic drug haloperidol that,

Received: November 26, 2013
Revised: April 14, 2014
Published: April 15, 2014

   dx.doi.org/10.1021/bi401575g | *Biochemistry* 2014, 53, 2993−3003

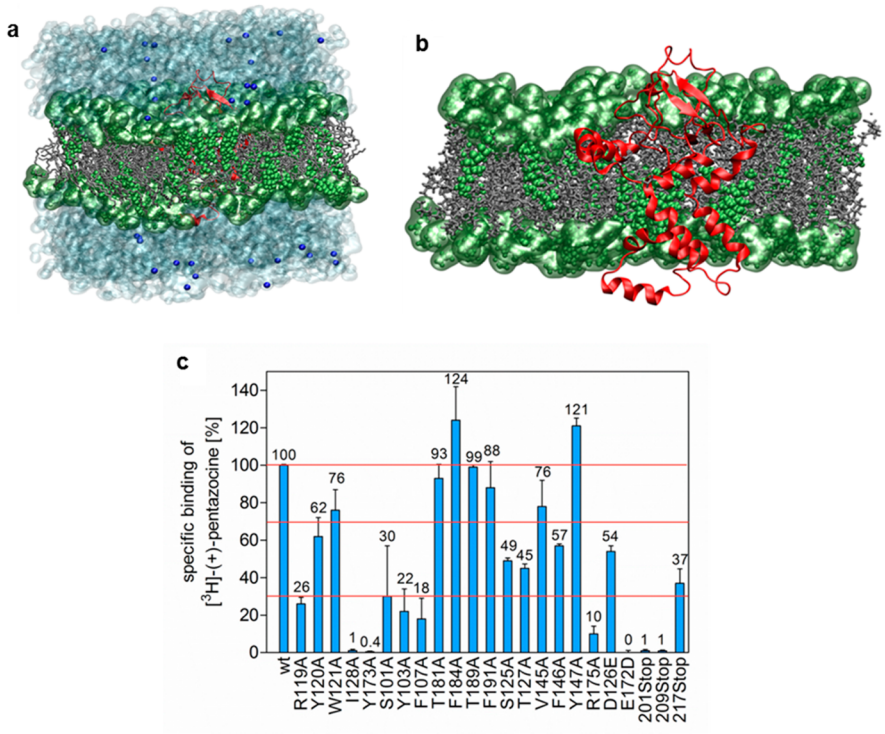

Figure 1. (a) 3D structure of the σ_1 receptor embedded in a 1-hexadecanoyl-2-[(9*Z*)-octadecenoyl]-*sn*-glycero-3-phosphocholine (POPC)/1-palmitoyl-2-oleoyl-*sn*-glycero-3-phosphoethanolamine (POPE)/cholesterol (2:2:1) membrane model. Water is shown with a light blue van der Waals surface, while some Cl^- and Na^+ ions are visible as dark blue spheres. The polar heads of POPC and POPE lipids are portrayed as forest green balls and sticks, with their solvent accessible surface area highlighted in transparent forest green. The lipid hydrophobic tails are shown as gray sticks. Cholesterol molecules are evidenced as light green CPK spheres, while the σ_1 receptor is depicted as a red ribbon. (b) Cross section of the system in panel a (water and ions not shown). (c) Specific [^{3}H]-(+)-pentazocine (PTZ) binding (SB) at a concentration of 40 nM to different alanine mutants of the human σ_1 receptor ($n \geq 2$). SB refers to the PTZ binding of the wild-type (wt) receptor (100%, first column). $^{**}p \leq 0.001$; $^{*}p \leq 0.01$. With respect to the red lines, SB < 30% indicates a strong influence of the particular amino acid on ligand binding, 30% ≤ SB ≤ 70% indicates a moderate influence on ligand binding, and SB > 70% indicates no influence on ligand binding.

however, shows poor selectivity as it also binds efficiently to several other receptors.[16]

From the structural standpoint, the available evidence concerns only the main structural motifs of the σ_1 receptor, which include an intracellular N-terminal end, two transmembrane-spanning domains (residues 10−30 and 80−100) linked by an extracellular loop, and a partially ordered C-terminal end.[17] A typical arginine-arginine ER locating signal near the N-terminal end has also been identified. Importantly, σ_1 receptors contain two GXXXG motifs, a signature that occurs frequently in membrane proteins that favor helix−helix interactions.[18] Because the σ_1 receptor is a membrane-bound protein, the process of its expression, purification, crystallization, and structure determination is difficult. Thus, no experimental data about the three-dimensional (3D) structure of the σ_1 receptor have been published.

Over the past two decades, site-directed mutagenesis,[19] photoaffinity labeling experiments,[20] and *in silico* homology modeling[21,22] have been performed to characterize the structure of the receptor and its binding site. According to these studies, a splice variant of the σ_1 receptor devoid of residues 119−149 (encoded by exon 3) is incapable of binding PTZ, 3-PPP, or haloperidol, while the receptor's N-terminal and C-terminal ends cannot bind ligands in the absence of either motif. The anionic amino acids D126 and E172 are essential for haloperidol binding, most likely via interaction with a cationic moiety of the ligand.[19] Replacement of residues S99, T103, L105, and L106, all belonging to the so-called steroid binding domain-like I (SBDLI), with alanine revealed that the Y103A mutation has the strongest influence on binding of both agonist (PTZ) and antagonist (NE-100) molecules. A difference in agonist and antagonist binding was detected in the case of the S99A/L105A/L106A triple mutant: while the level of NE-100 binding was reduced, the affinity of PTZ for the receptor was not affected. In subsequent investigations, the tyrosine residues at positions 173, 205, and 206 were also found to be important for cholesterol binding.[23−25] Intramolecular transfer of the photoaffinity label [^{125}I]IABM indicated that SBDLI and SBDLII of the σ_1 receptor are localized in juxtaposition. It was further suggested that the receptor first transmembrane motif (TMI), SBDLI, and SBDLII form the σ_1 ligand binding site, because the photoaffinity label [^{125}I]IAF was detected on both SBDLI and SBDLII after enzymatic digestion.[25] A photoactivated cocaine derivative was found to bind to D188.[20] Lastly, the binding was abolished when more than 15 amino acids of the C-terminal end were removed.[20] Recently, our group reported and validated the first 3D homology model of the σ_1 protein.[21,22] This 3D receptor model was used to characterize the ligand binding site of structurally unrelated σ_1 ligands and to identify key residues for protein−ligand interactions. According to the model, the protein structurally consists of two TM α-helices (spanning residues 10−30 and 80−100), a number of β-strands and an additional α-helix in the C-terminal half (residues 111−116, 133−135, 144−146, 158−164, and 180−200), and several loops (Figure 1a,b).

Aiming to improve our understanding of the structure and ligand binding of the σ_1 protein, we have conducted an extensive

dx.doi.org/10.1021/bi401575g | *Biochemistry* 2014, 53, 2993−3003

in vitro/*in silico* site-directed mutagenesis study of the receptor. Specifically, on the basis of preliminary *in silico* information, 23 mutants of the σ_1 receptor were cloned and expressed and their interactions with PTZ were assessed experimentally. Concomitantly, all direct and indirect effects exerted by the mutant residues on the receptor−agonist interactions could be reproduced *in silico* and were rationalized at the molecular level, thus casting new light on the binding site of this enigmatic receptor.

EXPERIMENTAL PROCEDURES

Site-Directed Mutagenesis and DNA Amplification. Plasmid pCMV6-AC-GFP containing the tGFP-tagged DNA of the human σ_1 receptor (OriGene Technologies) was used in all experiments. Point mutations or deletions were introduced with a QuikChange Lightning Site-Directed Mutagenesis Kit (Stratagene). All oligonucleotides that were used as primers to introduce the mutations were designed individually and purchased from Sigma-Aldrich. Site-directed mutagenesis was performed with a Mastercycler gradient (Eppendorf) using the parameters listed in Table S1 of the Supporting Information. For the degradation of parental DNA, 2 μL of Dpn I was added to the reaction mix and incubated for 10 min at 37 °C. DNA quantification and determination of purity were conducted by UV absorption measurement at 260 nm (BioPhotometer, Eppendorf). After Dpn I digestion, the mutated DNA was transformed into competent bacterial cells (*Escherichia coli* Top10F′) by the heat shock method. An adequate volume of DNA solution (equal to ∼1−2 μg of DNA) was added to 50 μL of the bacterial suspension. The mixture was incubated on ice for 40 min. Heat shock was performed for 60 s at 42 °C, followed by incubation on ice for 10 min. Subsequently, 300 μL of LB medium was added, and this mixture was incubated for 60 min at 37 °C. The bacterial cells were resuspended in the residual supernatant, streaked out on LBAmp/LBCarb (σ_1 wt and mutants) or LBKan (pEYFP-C1), and incubated at 37 °C for 14 h. DNA "Mini" preparation was performed to identify a clone that carries the plasmid DNA with the desired point mutation using the QIAprep Miniprep Kit (Quiagen). DNA "Maxi" preparation was performed to gain sufficient amounts of pure plasmid DNA for transfection with the Nucleobond Xtra Maxi Kit (Macherey-Nagel). Restriction analysis was performed to check if the correct DNA was extracted. The restriction enzymes EcoRI and XhoI of the FastDigest line with the FastDigest green buffer were used for the digestions of all other mutated plasmids (Fermentas). DNA sequences and point mutations were confirmed by professional sequencing (Primer T7). The sequencing was performed by GATC and checked with BLAST.

Cell Culture, Transient Transfection, and Expression of the Human σ_1 Receptor. Quail fibroblast cell line QT-6 (American Type Culture Collection) was used to express the native and modified human σ_1 receptor after transient transfection. Quail cells were used because of their high transfection efficiency. Moreover, in contrast to most of the human cells, quail cells do not express native σ_1 receptors. This property reflects the high signal-to-noise ratio, which is very important for generating reliable results. Indeed, the effects of mutations cannot be recorded selectively if a large amount of native σ_1 receptors is present. Moreover, quail cells have been used for the expression of various heterologous proteins in their active forms, including membrane proteins (e.g., human adenosine receptor subtype 2B). It is important to observe also that the σ_1 receptor of humans and quails is highly conserved. Therefore, it can be safely assumed that the mutant proteins do not behave differently in these two cell lines.

All working steps were performed in a Biowizard safety cabinet (Kojair Tech Oy). The adherent growing cells were cultivated in 75 cm^3 flasks with basal Iscove's medium containing 8% FBS, 2% chicken serum, 1% L-glutamine, and 1% penicillin/streptomycin at 37 °C with 5% CO_2 in a humidified atmosphere. For splitting, the cells were detached by incubation with an adequate volume of trypsin/EDTA for 5 min after a washing step with PBS to remove dead cells, cell fragments, and culture medium. Transient transfection was conducted by calcium phosphate coprecipitation. Prior to transfection, the cell split ratio was determined to achieve 50% confluence at the time of transfection. The DNA was precipitated overnight at −20 °C if applicable with an adequate volume of precipitation buffer [10 mM Tris (pH 7.8), 1 mM EDTA, and 300 mM NaCl]. The transfection was conducted with 12.5 μg of plasmid DNA containing the native or modified human σ_1 receptor per cell culture flask (75 cm^2). Four flasks or dishes were used per mutation. For each series of transfections, the wild-type DNA was transfected on the same day with the same reagents as the positive control. As a negative control, the cells were treated in the same way as the transfected cells but without DNA. The reagent mix contained 12.5 μg of plasmid DNA, 2 μg of a plasmid containing the YFP gene as control of the transfection efficiency, 62 μL of 2 M calcium chloride, and as much as water needed to yield to a volume of 500 mL. The mixture was added dropwise and slowly into 500 μL of 2× HBS (pH 7.13) (280 mM NaCl, 1.5 mM $Na_2HPO_4 \cdot 2H_2O$, and 50 mM HEPES) during vortexing. This transfection mix was added slowly to the medium of the adherent growing QT-6 cells and was dispersed well. Incubation was performed at 37 °C with 5% CO_2. Three to four hours after transfection, a glycerine shock of the cells was performed. Therefore, the medium was removed, and 2 mL of a cold glycerine shock [15% (v/v) glycerine and 2× 50% HBS] solution was added to the cells. The cells were incubated for 2 min with this solution while being continuously gently shaken at room temperature. After the removal of the glycerine shock solution and one washing step with cold PBS, new medium was added to the cells, and they were incubated for 24 h at 37 °C with 5% CO_2.

Preparation of the Receptor Material. For the preparation of the receptor material of the transfected and untransfected cells, the medium was removed and the cells were washed with cold PBS buffer. PBS (2 mL) was added; the cells were detached with a cell scraper, and the suspension was collected in a centrifugation tube. PBS buffer (3 mL) was used to wash the flask and to collect the residual of the detached cells. The cells were pelleted by centrifugation with Hettich Rotina 35R (4000 rpm for 15 min at 4 °C), resuspended for cell counting, and again centrifuged. The final pellet was resuspended in a defined volume of Tris buffer (pH 7.4, 50 mM) to achieve a standardized suspension containing 3000000 cells/mL. The cells were lysed and homogenized by sonication at volumes between 5 and 15 mL (3 × 10 s cycles with intercepts of 10 s), and the membrane fragment suspension was stored at −80 °C (3000000 cells/mL in a volume of 5−15 mL).

Analysis of Protein Expression. The Lowry protein determination method[26] was used to verify equal amounts of total protein in the different receptor preparations. Homogeneous amounts of the σ_1 receptor in each receptor preparation were proved by specific antibody staining of a Western Blot after sodium dodecyl sulfate−polyacrylamide gel electrophoresis (SDS−PAGE). Equal transfection efficiencies were controlled

by the visualization of YFP on the Western blot; 250 μL of the receptor preparation was centrifuged (5000 rpm for 10 min at 4 °C, Eppendorf centrifuge 5417R), and the pellet was resuspended in 20 μL of H_2O. Ten microliters of lysis buffer (pH 6.8) [130 mM Tris base, 10% (w/v) SDS, 10% (v/v) 2-mercaptoethanol, 20% (v/v) glycerine, and 0.06% (w/v) bromophenol blue] was added, and the samples were digested for 10 min at 95 °C. SDS−PAGE with a Mini-PROTEAN Tetra Electrophoresis System filled with running buffer (3.02 g/L Tris base, 18.8 g/L glycine, and 1 g/L SDS) was performed at 100 V until the proteins passed the stacking gel. Then the voltage was set to 160 V. The Mini-PROTEAN Tetra Electrophoresis System with a Mini Trans-Bot Module was employed for the wet blotting method. The blotting chamber was filled with 1 L of transfer buffer (pH 8.3) (3.03 g/L Tris base and 14.4 g/L glycine) containing 20% MeOH. The system was cooled with ice during the blotting procedure. Blotting was performed for 1 h at 100 V. The blot was incubated with a blocking solution [5% (w/v) milk powder and 0.05% (v/v) Tween 20 in PBS] for 1 h at room temperature. This step was followed by incubation with the first antibody for 14 h or for a minimum of 3 h (OPRS1 antibody, rabbit, Abcam; GFP antibody, mouse, Roche Diagnostics; tGFP antibody, rabbit, Evrogen). After the blot had been washed with washing buffer [0.05% (v/v) Tween 20 in PBS] for 4 × 10 min, it was incubated with the second, HRP-coupled antibody (ECLTM anti-rabbit IgG from donkey and ECLTM anti-mouse IgG from sheep, Amersham Biosciences) for 1 h and washed again with washing buffer (4 × 10 min). Thereafter, the blot was incubated for 2 min with a 1:1 mixture of detection reagent 1 peroxide solution and 2 luminol enhancer solution (Thermo Scientific) to start the luminescence reaction. Horseradish peroxidase, which is coupled to the secondary antibody, catalyzes the oxidation of luminol in the presence of H_2O_2. Luminescence detection of the oxidized luminol was performed with a Cawomat 2000 IR instrument (Cawo Photochemische Fabrik) and an Intas ChemoCam Imager (Intas Science Imaging Instruments).

Laser Scanning Microscopy. Transfection was conducted with 5 μg of DNA per well by calcium phosphate coprecipitation as described above. After 24 h, cells were fixed by incubation with paraformaldehyde for 30 min and mounted on slides using Entellan (Merck) as the mounting medium. The 63× oil objective for use with immersion oil was employed for the observations. Images were recorded with laser excitation at 488 nm, and emission was registered from 500 to 600 nm (Leica TCS SP2 laser scanning microscope, Leica Microsystems).

Binding Experiments. In the saturation experiments, nonspecific binding and total binding were measured at increasing concentrations of radioligand [^{3}H]-(+)-pentazocine. Assay concentrations of 0.5, 1, 2, 3, 5, 10, 20, 40, and 60 nM [^{3}H]-(+)-pentazocine were incubated for 2 h at 37 °C while the samples were being continuously shaken (400 rpm) in a total reaction volume of 200 μL. Besides 50 μL of the radioligand, the reaction mixture contained 50 μL of the membrane preparation (approximately 150000 cells/well). For the determination of nonspecific binding, it contains a further 50 μL of Tris buffer (pH 7.4, 50 mM) and 50 μL of haloperidol (40 μM). For the determination of total binding, 100 μL of Tris buffer was added. The incubation process was terminated by filtration using filter mats (PerkinElmer), which were presoaked in 0.2% aqueous polyethylenimine for 2 h at room temperature. Each well was washed eight times with 300 μL of water at room temperature. The filter mats were dried, and a solid scintillator (MeltiLex B/HS, PerkinElmer) was melted on the filter mat at 95 °C. After solidification, the bound radioactivity was counted in the scintillation analyzer (Wallac MicroBeta TriLux, PerkinElmer) with an overall counting efficiency of 20%. The total and nonspecific binding was assessed repeatedly as described above but only at a [^{3}H]-(+)-pentazocine concentration of 40 nM with the same parameters described above. The specific radioligand binding of mutated receptors is given as the percent of radioligand binding of the wild-type σ_1 receptor.

Data Analysis. Analysis of the binding data was performed with SigmaPlot 11, 12 (Systat Software) and GraphPad Prism (version 5.02, GraphPad Software). Analysis of the saturation experiments was conducted by nonlinear regression using the "one-site-saturation" calculation method.

Membrane/Protein Model Generation. The CHARMM-GUI Lipid Builder web application[27,28] was used to insert our σ_1 3D model[21] into a pre-equilibrated membrane. The membrane was built using 1-palmitoyl-2-oleoyl-*sn*-glycero-3-phosphocholine (POPC), 1-palmitoyl-2-oleoyl-*sn*-glycero-3-phosphoethanolamine (POPE), and cholesterol in a 2:2:1 ratio; 125 and 115 lipid molecules constituted the top and bottom membrane leaflets, respectively. Both sides of the membrane were solvated by two layers of a 0.150 M NaCl solution of TIP3P water molecules,[29] each extending 20 Å from the membrane lipid polar heads. The entire system was parametrized using the lipid11[30] and ff03[31] force fields for the lipids and the protein, respectively. After an initial relaxation (for details, see the Supporting Information), the systems was allowed to equilibrate for 50 ns adopting a semi-isotropic constant surface tension of 15.0 dyn/cm. Once an equilibrated value of area per lipid was reached, all remaining constraints were finally released, and MD NPT simulations were performed for an additional 50 ns. At the end of the MD simulation, we took the final snapshot and separated the protein from the membrane. Then, we used this optimized protein structure as the starting conformation for the subsequent docking studies.

Docking Studies. The model structure of PTZ was sketched and geometrically optimized using Discovery Studio (DS, version 2.5, Accelrys Inc., San Diego, CA). The optimized structure of PTZ was then docked into the σ_1 putative binding pocket by applying a consolidated procedure.[21,22,32−34] All docking experiments were performed with Autodock 4.3/Autodock Tools 1.4.6 on a win64 platform (for details, see the Supporting Information).

Molecular Dynamics Simulations. The ligand−receptor complex obtained from the docking procedure was further reinserted into the membrane and subsequently refined in Amber 12[35] as follows. Each system was relaxed by 500 steps of steepest descent followed by 500 other conjugate gradient minimization steps and then gradually heated to a temperature of 300 K in intervals of 50 ps of *NVT* MD, using a Verlet integration time step of 1.0 fs. The Langevin thermostat was used to control temperature, with a collision frequency of 2.0 ps^{-1}. The SHAKE method[36] was used to constrain all of the covalently bound hydrogen atoms, while long-range nonbonded van der Waals interactions were truncated by using dual cutoffs of 6 and 12 Å. The particle mesh Ewald (PME) method was applied to treat long-range electrostatic interactions. All simulations were conducted with periodic boundary conditions. The density of the system was subsequently equilibrated via MD runs in the *NPT* ensemble, with isotropic position scaling and a pressure relaxation time of 1.0 ps, for 50 ps with a time step of 1 fs. Each system was further equilibrated using *NPT* MD runs at 300 K, with a pressure relaxation time of 2.0 ps. Three equilibration

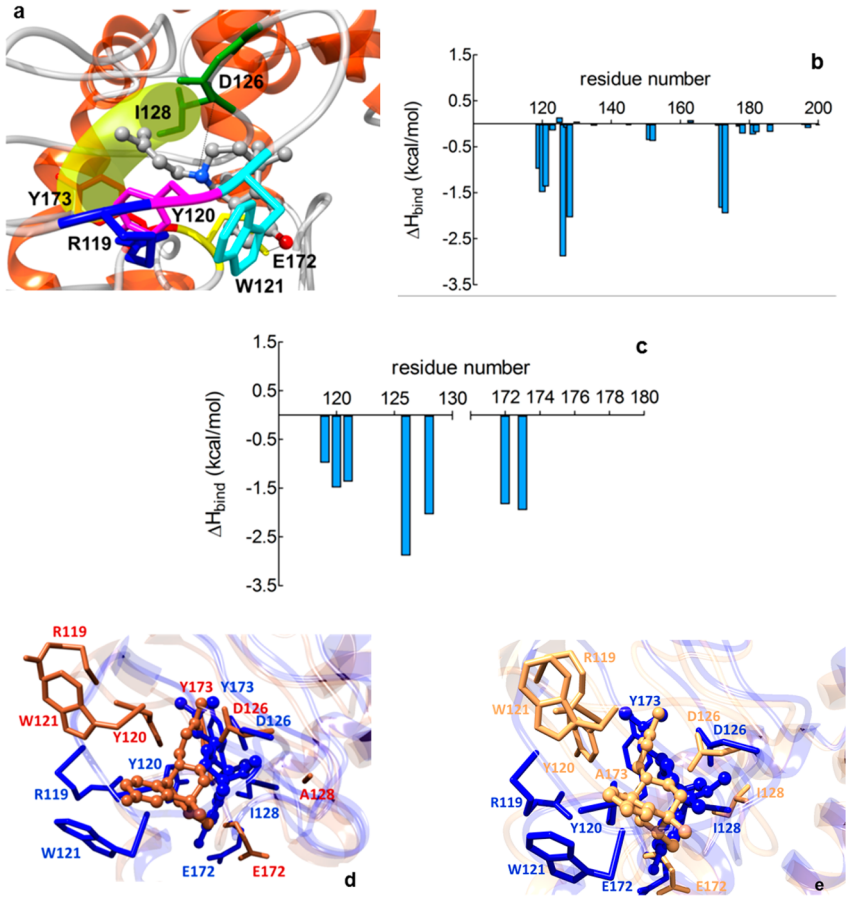

Figure 2. (a) Equilibrated MD snapshot of the wt σ_1 receptor in complex with PTZ. The image is a close-up of the receptor binding site. The ligand is shown with colored balls and sticks (C, gray; N, blue; O, red). The protein residues mainly involved in the interaction with PTZ are highlighted as labeled colored sticks. Salt bridges and H-bond interactions are shown as solid and dotted black lines, respectively. The yellow shadow denotes the hydrophobic pocket generated by the side chains of I128 and Y173. (b) Per residue energy decomposition for the wt σ_1 receptor in complex with PTZ. Only σ_1 amino acids from position 100 to 200 are shown, as for all remaining residues the contribution to ligand binding is irrelevant. (c) Expanded view of panel b showing those σ_1 residues for which $|\Delta H_{bind}| \geq |0.5$ kcal/moll. Comparison of the equilibrated MD snapshots of the wt σ_1 receptor (blue) with (d) I128A (sienna) and (e) Y173A (sandy brown) mutants in complex with PTZ. The ligand is shown as balls and sticks colored according to the respective protein complex. In panels a, d, and e, hydrogen atoms, water molecules, ions, and counterions were omitted for the sake of clarity.

steps were performed, each 2 ns long with a time step of 2.0 fs. To check the system stability, the fluctuations of the root-mean-square deviation (rmsd) of the simulated position of the backbone atoms of the σ_1 receptor with respect to those of the initial protein were monitored. All chemicophysical parameters and rmsd values showed very low fluctuations at the end of the equilibration process, indicating that the systems reached a true equilibrium condition. The equilibration phase was followed by a data production run consisting of 15 ns of MD simulations in the *NVT* ensemble. Only the last 10 ns of each equilibrated MD trajectory was considered for statistical data collections.

Free Energy of Binding Analysis. The binding free energy, ΔG_{bind}, between PTZ and the σ_1 receptor was estimated by resorting to the MM/PBSA approach.[37] According to this well-validated methodology,[21,22,32−34,38] the free energy was calculated for each molecular species (complex, receptor, and ligand), and the binding free energy was computed as the difference (for details, see the Supporting Information).

A per residue binding free energy decomposition was performed exploiting the MD trajectory of each given compound−receptor complex, with the aim of identifying the key residues involved in the ligand−receptor interaction. This analysis was conducted using the MM/GBSA approach[39,40] and was based on the same snapshots used in the binding free energy calculation.

Computational Mutagenesis. For the computational mutagenesis studies, mutation of the selected residues to alanine was performed on the membrane-bound equilibrated structure of the wild-type σ_1 receptor complex. Each mutated complex was equilibrated in a 0.150 M NaCl TIP3P water solution to relax eventual conformational perturbations induced by mutation of the residue. Each system was then first subjected to 100 energy minimization steps, followed by further solvent equilibration for 100 ps of MD at 310 K. Finally, the entire system was equilibrated for 2 ns at 310 K. The subsequent MD simulation was conducted with Amber 12 as described above.

Computational Resources. All simulations were conducted using the Pmemd modules of Amber 12, running on a single GPU on a EURORA calculation cluster of the CINECA supercomputer facility (Bologna, Italy). The entire MD simulation and data analysis procedure was optimized by integrating Amber 12 in modeFRONTIER,[41] a multidisciplinary and multiobjective optimization and design environment.

dx.doi.org/10.1021/bi401575g | *Biochemistry* 2014, 53, 2993−3003

RESULTS AND DISCUSSION

On the basis of preliminary *in silico* information, 23 mutants of the σ_1 receptor were cloned and expressed and their interactions with PTZ were assessed experimentally (Figure 1c). As described below, all direct and indirect effects exerted by the mutant residues on the receptor−agonist interactions could be reproduced *in silico* and rationalized at the molecular level (Table S3 of the Supporting Information).

At first, we considered those σ_1 residues to belong to the protein putative ligand binding site. For this purpose, the interaction of PTZ with the wild-type (wt) σ_1 receptor 3D model was simulated using molecular dynamics (MD): the corresponding estimated drug−receptor affinity (K_i^c) value of 45 nM (Table S4 of the Supporting Information) compares well with the experimentally measured K_i^e value of 15 nM.[19] Specifically, the following interactions were found to be essential for PTZ binding (Figure 2a): (i) a permanent salt bridge between the NH^+ moiety of PTZ and the COO^- group of D126 [average dynamic length (ADL) of 3.93 ± 0.09 Å], (ii) a stable hydrogen bond between the carboxylate group of E172 and the hydroxyl substituent of PTZ (ADL of 1.98 ± 0.04 Å), (iii) a T-stacking $\pi-\pi$ interaction between the side chains of Y120 and W121 and the heteroaromatic condensed rings of PTZ, and (iv) highly stabilizing van der Waals and electrostatic interactions between R119, I128, and Y173 and the aliphatic/aromatic portions of the ligand. These receptor−ligand interactions were quantified via a per residue deconvolution of the free energy of binding (Figure 2b,c). Accordingly, the salt bridge and the hydrogen bond involving D126 and E172 are responsible for stabilizing contributions of −2.89 and −1.83 kcal/mol, respectively. Substantial van der Waals and electrostatic interactions are further contributed by R119 (−0.98 kcal/mol), Y120 (−1.49 kcal/mol), W121 (−1.37 kcal/mol), I128 (−2.04 kcal/mol), and Y173 (−1.95 kcal/mol). T151 and V152 additionally contribute −0.36 and −0.38 kcal/mol, respectively, to the stabilization of PTZ−σ_1 binding.

Interestingly, in a recent work, Chu at al. discussed the possibility of σ_1 receptors existing in a homo- or heterodimeric form when bound to a single ligand.[42] Specifically, these authors suggested that the observed σ_1 binding and activity of the *N*-[3-(4-nitrophenyl)propyl]alkan-1-amine 4-NPPC12 might evoke a ligand binding model for the σ_1 receptor that likely involves a receptor dimer and/or oligomer. Undoubtedly, more conclusive studies are needed to conclusively ascertain this interesting hypothesis and to discard specific ligand-dependent oligomerization mechanisms. On the other hand, the monomeric 3D model of the σ_1 receptor discussed in this work has been comprehensively employed to predict and rationalize the binding modes and affinities of a broad series of structurally unrelated σ_1 ligands, including PTZ, and the results of these *in silico* predictions were successfully validated against relevant experimental data. Therefore, should a dimeric ligand-bound form of the σ_1 receptor be verified for different, known σ_1 ligands,[21,22,32−34] the present monomeric σ_1−ligand binding model may eventually constitute a step along the dimerization pathway.

R119, I128, and Y173 Are Essential Residues for PTZ Binding. The results of the site-directed mutations of those residues identified *in silico* as being crucial for PTZ binding are listed in Table 1. We see that mutating residues R119, I128, and Y173 within the σ_1 binding site to alanine leads to an almost complete loss of ligand binding, as predicted from simulation (Table 1, Figures 1c and 2d,e, and Figure S4 of the Supporting Information). Indeed, residues I128 and Y173 afford a significant contribution to the PTZ−σ_1 complex (Figure 2c), as their side chains generate a hydrophobic pocket tailored to encase the methylbut-2-enyl moiety of PTZ (Figure 2d,e). Accordingly, the favorable hydrophobic interactions exerted by these two residues in the binding of PTZ are lost upon alanine substitution [for I128, SB = 1% and $\Delta\Delta G_{bind}$ = −2.47 kcal/mol; for Y173, SB = 0.4% and $\Delta\Delta G_{bind}$ = −2.70 kcal/mol (Figure 1c)]. On the other hand, the affinity of the Y120A and W121 σ_1 mutants for PTZ was only partly reduced (SB values of 62 and 76%, respectively). Interestingly, the relevant modeling analysis reveals that, although each of these two aromatic residues concurs in stabilizing PTZ binding mainly via $\pi-\pi$ interactions (Figure 2c and Figure S4 of the Supporting Information), the effect of mutating either of these two positions to alanine results in an apt rearrangement of the alternative residue side chain within the binding site and, hence, in a partial compensation of the receptor affinity loss [$\Delta\Delta G_{bind}$ values of −0.68 kcal/mol for Y120A and −1.54 kcal/mol for W121A (Table 1)].

Table 1. *In Vitro/in Silico* Site-Directed Mutagenesis of σ_1 Residues Directly Involved in PTZ Binding[a]

σ_1 residue	specific binding of PTZ (%)	ΔG_{bind} (kcal/mol)	$\Delta\Delta G_{bind}$[b] (kcal/mol)
wt	100	−10.02 (0.05)	−
R119A	26 (3.5)	−8.31 (0.05)	−1.71
Y120A	62 (10)	−9.34 (0.08)	−0.68
W121A	76 (12)	−8.48 (0.06)	−1.54
I128A	1.1 (0.6)	−7.55 (0.06)	−2.47
Y173A	0.4 (0.4)	−7.32 (0.11)	−2.70
D126E	54 (3)	−9.13 (0.07)	−0.89
E172D	0 (0.1)	−7.88 (0.06)	−2.14

[a]Specific PTZ binding of different alanine mutants of the human σ_1 receptor and *in silico* estimated free energy of binding (ΔG_{bind}) of the same σ_1 alanine mutants as generated by computational mutagenesis. Errors are given in parentheses as standard errors of the mean. [b]$\Delta\Delta G_{bind} = \Delta G_{bind,wt} - \Delta G_{bind,mutant}$. By definition, a negative value of $\Delta\Delta G_{bind}$ indicates a favorable contribution for the wt residue in that position and vice versa.

D126 and E172 Are Strategically Located within the σ_1 Binding Site. The anionic amino acids D126 and E172 are known to be essential for ligand (i.e., haloperidol) binding,[19] and our combined study indeed confirms their role in binding PTZ (Figures 1c and 2b,c). To substantiate this prediction, however, we decided to swap these two residues with each other instead of replacing them with alanine in the corresponding site-directed mutagenesis experiments. Interestingly, the E172D σ_1 mutant was totally devoid of PTZ binding, while the D126E isoform preserved 54% of the wt affinity. These results clearly demonstrate the specific and strategic location of these two negative charges within the σ_1 binding site: while the elongation of the side chain from aspartate to glutamate at position 126 is somewhat tolerated [$\Delta\Delta G_{bind}$ = −0.89 kcal/mol (Table 1)], resulting in a mild rearrangement of the protein binding pocket that preserves the main network of interactions between the ligand and the protein, the corresponding reduction in chain length in the E172D mutant fully abrogates the ability of the protein to bind the radioligand [$\Delta\Delta G_{bind}$ = −2.14 kcal/mol (Table 1)]. In detail, the substitution of D/E at position 126 leads to a longer, and hence less stable, salt bridge between the NH^+ group ion of PTZ and the COO^- group of the E126 side chain (ADL of 4.85 ± 0.08 Å), leaving all other ligand−receptor

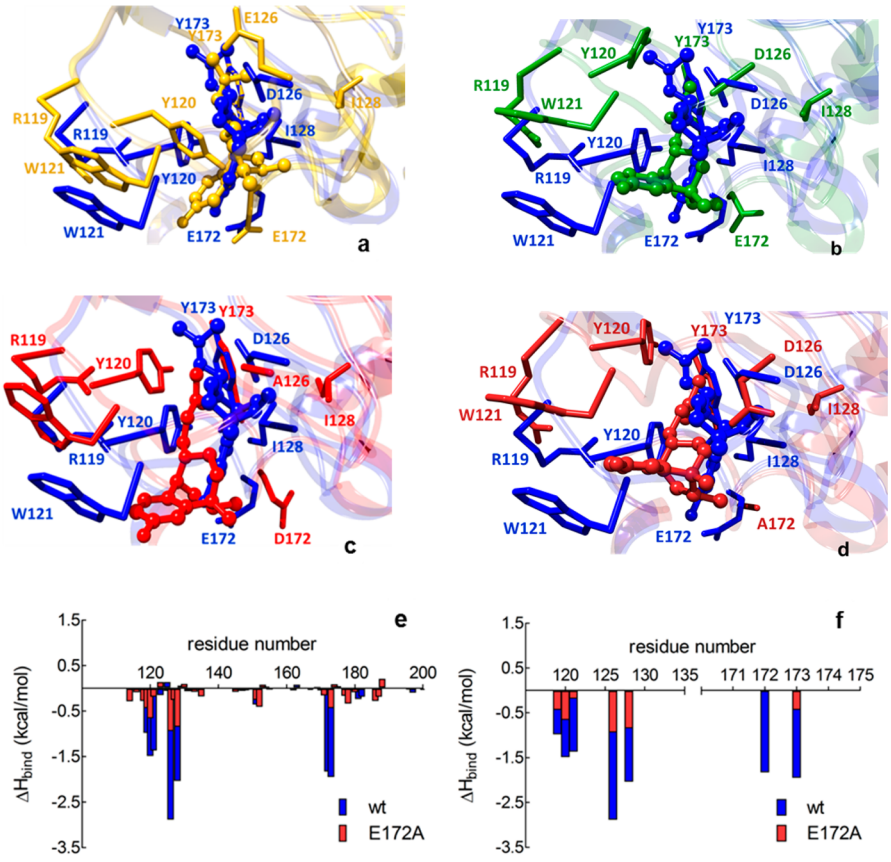

Figure 3. Comparison of the equilibrated MD snapshots of the wt σ_1 receptor (blue) with (a) D126E (goldenrod), (b) E172D (forest green), (c) D126A (red), and (d) E172A (firebrick) mutants in complex with PTZ. The images are close-ups of the receptor binding site. The ligand is shown as balls and sticks colored according to the respective protein complex. In panels a–c, hydrogen atoms, water molecules, ions, and counterions were omitted for the sake of clarity. (e) Comparison of σ_1 residue contributions to PTZ binding for the wt and the E172D mutant protein. (f) Expanded view of panel e showing those σ_1 residues for which $|\Delta H_{bind}| \geq |0.5$ kcal/moll in the wt receptor.

interactions almost unaltered (Figure 3a). Upon E172D substitution, however, the missing H-bond between position 172 and the OH group on PTZ leads to a global readjustment of the protein binding site (Figure 3b), which ultimately leads to an overall decrease in the favorable contributions to ligand binding.

To further corroborate this fundamental finding, we also performed *in silico* mutagenesis of D126 and E172 to alanine. As expected, the prominent role exerted by D126 and E172 in binding PTZ is reflected in the highly unfavorable affinity predicted for the D126A and E172A mutants [$\Delta\Delta G_{bind}$ values of −3.01 and −2.02 kcal/mol, respectively (Table S3 of the Supporting Information)]. The missing critical salt bridge and H-bond interactions in which these residues are engaged in the wt protein bound to PTZ result in a catastrophic loss of drug interaction when the residues are mutated to alanine (Figure 3c–f). These predictions match the results previously reported by Seth et al.[19] for *in vitro* PTZ binding assays of the D126G and E172G σ_1 mutants; taken together, these results ultimately confirm the obligatory nature of the highly conserved D126 and E172 residues for the ligand binding function of the σ_1 receptor.

Polar Residues Are Required in the SBDLI Domain To Maintain the Binding Site Geometry. Next, we explored the effect of mutations on residues belonging to the SBDLI and SBDLII σ_1 domains by performing a systematic substitution of the polar (S and T) and aromatic (F and Y) amino acids of these protein regions with alanine. The results are listed in Table 2. Mutating the polar and aromatic amino acids of SBDLI (S101, Y103, and F107) to alanine both *in silico* and *in vitro* led to a considerable decrease in the level of PTZ binding [SB = 18–30%, and $\Delta\Delta G_{bind} = -2.13$ to −1.86 kcal/mol (Table 2, rows 1–3)]. A sensible explanation of these results is that all three alanine-mutated residues are in the proximity of the transmembrane domain of the σ_1 receptor (Figure 4a) and, during the long MD simulation, they promote a substantial modification of both the

Table 2. *In Vitro*/*in Silico* Site-Directed Mutagenesis of σ_1 Residues Belonging to the SBDLI and SBDLII Motifs[a]

σ_1 residue	domain	specific binding of PTZ (%)	ΔG_{bind} (kcal/mol)	$\Delta\Delta G_{bind}$[b] (kcal/mol)
S101A	SBDLI	30 (27)	−8.16 (0.08)	−1.86
Y103A		22 (12)	−7.89 (0.09)	−2.13
F107A		18 (11)	−8.05 (0.05)	−1.97
T181A	SBDLII	93 (7.5)	−9.99 (0.11)	−0.03
F184A		124 (18)	−10.55 (0.07)	0.53
T189A		99 (1.1)	−9.87 (0.07)	−0.15
F191A		88 (14)	−9.13 (0.10)	−0.89
201Stop		1.0 (0.6)	–	–
209Stop		0.9 (0.5)	–	–
217Stop		37 (7.7)	−8.80 (0.06)	−1.22

[a]Specific PTZ binding of different alanine mutants of the human σ_1 receptor and *in silico*-estimated free energy of binding (ΔG_{bind}) of the same σ_1 alanine mutants as generated by computational mutagenesis. Errors are given in parentheses as standard errors of the mean. [b]$\Delta\Delta G_{bind} = \Delta G_{bind,wt} - \Delta G_{bind,mutant}$.

dx.doi.org/10.1021/bi401575g | *Biochemistry* 2014, 53, 2993–3003

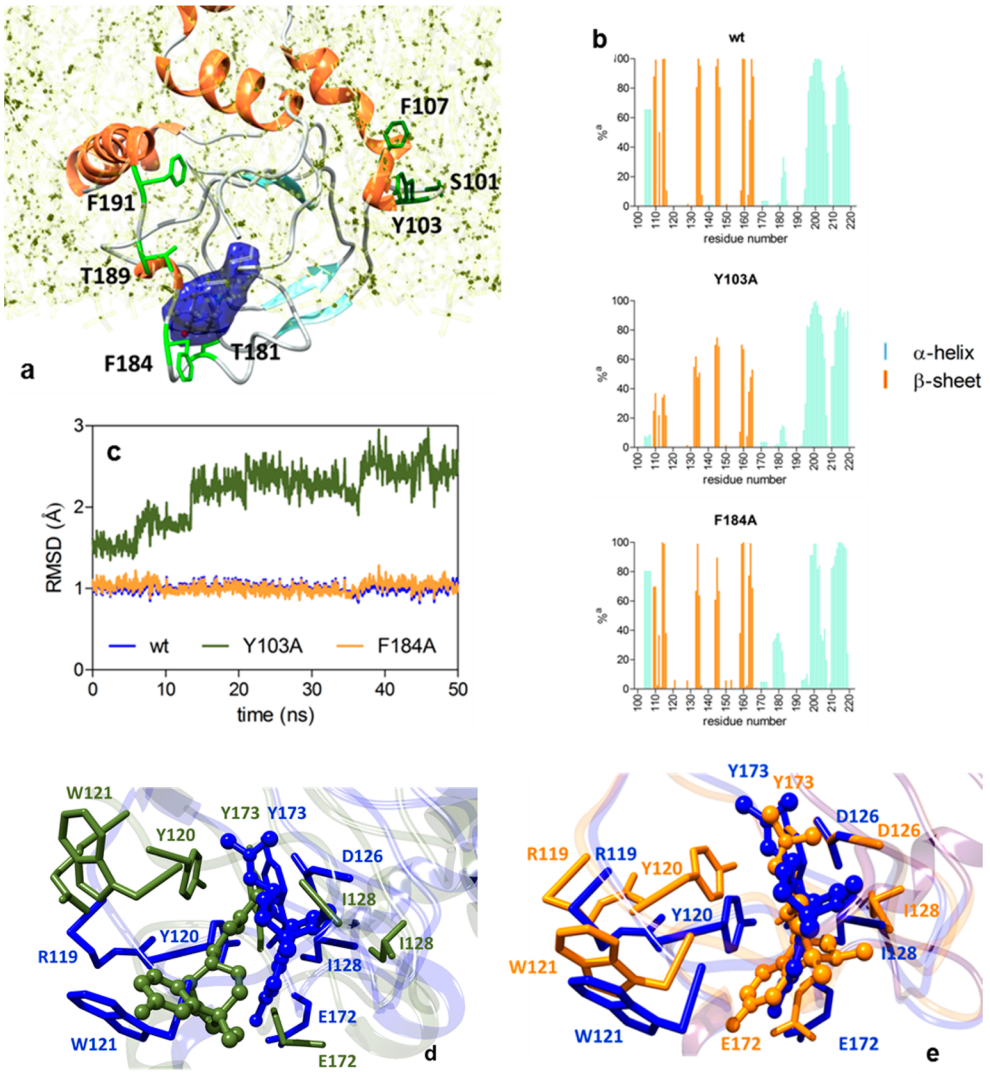

Figure 4. (a) Close-up the residues belonging to the σ_1 SBDLI and -II domains, represented as forest and light green sticks, respectively. The ligand is shown as element-colored balls and sticks (C, gray; N, blue; O, red) with its van der Waals surface colored blue. The membrane phospholipids are portrayed as semitransparent light yellow balls and sticks. (b) General secondary structure description of the σ_1 receptor (amino acids 100−223) during MD simulations of the wt−, Y103A−, and F184A−PTZ complexes. The *y*-axis gives the percentage of specific secondary structure for each σ_1 residue. (c) rmsd values of the coordinates of the heavy atoms of PTZ along the MD simulation compared with those of the initial structure. Comparison of the equilibrated MD snapshots of the wt σ_1 receptor (blue) with (d) Y103A (dark olive green) and (e) F184A (orange) mutants in complex with PTZ. The images are close-ups of the receptor binding site. The ligand is shown as balls and sticks colored according to the respective protein complex. In panels d and e, hydrogen atoms, water molecules, ions, and counterions were omitted for the sake of clarity.

entire binding site and the surrounding protein regions. Taking the PTZ−σ_1(Y103A) complex as a proof of concept, we observed a different rearrangement of the secondary structure of this protein portion with respect to the PTZ−wt assembly (Figure 4b, top and central panels), ultimately resulting in an expansion of the receptor binding pocket from an average dynamic volume (ADV) of 509 ± 5 Å^3 to an ADV of 573 ± 7 Å^3. Accordingly, the ligand binds the receptor more loosely, as its interactions with the protein residues lining the binding site become weaker (Figure 4c). This effect is clearly seen in the behavior of the rmsd of the heavy atom of PTZ during the MD simulation (Figure 4d): after equilibration, the ligand assumes a stable conformation in the wt binding pocket with an average rmsd of 1.01 ± 0.06 Å, while a larger rmsd fluctuation (2.18 ± 0.35 Å) and a longer time to equilibrium are observed for the Y103A mutant σ_1−PTZ complex.

Residues in the SBDLII Domain Scarcely Contribute to Ligand Binding. In stark contrast, analogous mutations in the SBDLII domain barely influenced PTZ binding, if they did at all [SB = 93−100%, and $\Delta\Delta G_{bind}$ = −0.59 to −0.03 kcal/mol (Table 2, rows 4−7)]. A comparison of the membrane-bound wt and SDBLII mutated σ_1 isoforms reveals that the presence of mutations at the SBDLII domain does not lead to substantial alteration of both the membrane and the protein binding site and/or overall structure. Indeed, in the representative example of the PTZ−σ_1(F184A) complex, the fingerprint of the protein secondary structure is conserved (Figure 4b, top and bottom panels) and the average dynamic volume is essentially unchanged (507 ± 7 Å^3). Moreover, PTZ maintains a very stable conformation in the binding site during the entire MD simulation, as substantiated by the relevant rmsd [1.01 ± 0.07 Å (Figure 4c)]. Lastly, all ligand−receptor interactions detected for the wt complex are maintained in this as well as in all other

dx.doi.org/10.1021/bi401575g | *Biochemistry* 2014, 53, 2993−3003

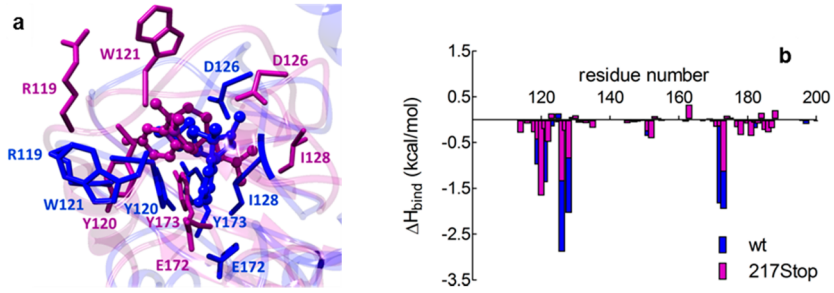

Figure 5. *In silico* mutagenesis of σ_1 receptor residues via deletion of the seven-residue YLFGQDP sequence from the protein C-terminal domain. (a) Comparison of the equilibrated MD snapshots of the wt (blue) and C-terminal seven-residue-truncated σ_1 receptor (magenta) in complex with PTZ. The image is a close-up of the receptor binding site. The ligand is shown as balls and sticks colored according to the respective protein complex. Hydrogen atoms, water molecules, ions, and counterions were omitted for the sake of clarity. (b) Comparison of contributions of σ_1 receptor residues to PTZ binding for the wt and C-terminal seven-residue-truncated protein.

SBDLII mutated complexes examined with no significant differences in binding mode or strength (Figure 4e). Remarkably, in a previous study, SBDLII was postulated to be part of the σ_1 ligand binding site.[25] Our results clearly do not support this hypothesis. It has been further proposed that SBDLII is responsible for anchoring the σ_1 receptors to the membrane and, in so doing, stabilizing the 3D structure of the protein. Once again, our combined *in vitro*/*in silico* experiments point in the opposite direction. Taken together, our findings lead to the conclusion that, while the SBDLI domain is part of the binding site of the σ_1 receptor and, as such, mutations at this domain lead to a drastic decrease in receptor−ligand affinity, the SBDLII domain does not belong to the σ_1 ligand binding site. Accordingly, mutations in this protein domain exert only a marginal effect on ligand binding, if any at all.

Even Small Deletions in the σ_1 C-Terminal End Abrogate Ligand Binding. As briefly mentioned above, σ_1 ligand binding is abrogated when more than 15 amino acids are removed from the C-terminal end of the protein.[20] Thus, we further investigated this aspect by deleting 7, 15, and 23 amino acids from the C-terminal end of the σ_1 receptor and determined the affinity of the truncated receptors for PTZ. As expected, elimination of 15 and 23 amino acids resulted in the loss of PTZ binding ability (Figure 1c and Table 2). More interestingly, also, the removal of only seven residues from the receptor C-terminal end led to a considerable decrease in the level of PTZ binding (SB = 37%). Again, these experiments were rationalized by the corresponding *in silico* assays. While the major deletions resulted in a partially unfolded structure of the receptor missing a large portion of the ligand binding site, the affinity of the seven-residue-truncated protein for PTZ remained low (Figure 5a), as quantified by the ΔG_{bind} value of −8.80 kcal/mol. The corresponding $\Delta\Delta G_{bind}$ of −1.22 kcal/mol nicely correlates with the 63% decrease in affinity with respect to that of the wt protein reported by *in vitro* mutagenesis. The seven deleted amino acids are not directly involved in ligand binding; however, the missing YLFGQDP sequence results in a structural modification of the receptor that, like a domino effect, propagates along the protein backbone to the binding site (Figure 5b). This overall configuration rearrangement directly affects three σ_1 residues most important for ligand binding: R119, D126, and E172. Specifically, the interaction of D126 with PTZ becomes less favorable by 1.54 kcal/mol with respect to the wt isoform, while E172 decreases its contribution by −1.68 kcal/mol.

Distal Residues Also Shape the σ_1 Binding Site. Lastly, to determine whether other σ_1 receptor residues could play a critical role in binding PTZ, several alternative positions between the SBDLI and -II protein domains were substituted with alanine. *In silico* mutagenesis results suggested that the hydrophobic V145 and the aromatic F146 and Y147 residues, when mutated to alanine, result in minor (if any) changes in the protein binding site conformation (Table 3). These results are confirmed by the corresponding *in vitro* experiments, showing that for these three residues the SB values range between 57 and 121%. However, the alanine mutants of the basic amino acid R175 and of the two polar residues (S125 and T127) show a moderate (S125A and T127A) to strong (R175A) influence on PTZ binding, as revealed by the drastically less favorable $\Delta\Delta G_{bind}$ values of −1.45, −1.24, and −2.02 kcal/mol, respectively (Table 3), and supported by the corresponding SB values (49, 45, and 10%, respectively). The S145A and T127A mutations transform the environment in the proximity of the negatively charged D126 from polar to hydrophobic that, in turn, decreases the strength of its salt bridge with PTZ (ADL values of 4.76 ± 0.07 and 4.69 ± 0.10 Å for S145A and T127A, respectively). The case of the R175A mutant is more complex, as experiments detect a drastically reduced affinity of this mutant σ_1 isoform for PTZ (SB = 10%). The calculated free energy of binding differs considerably from that of the wt σ_1 complex ($\Delta\Delta G_{bind}$ = −2.02 kcal/mol), although this residue is not directly involved in PTZ binding. Importantly, however, along the entire MD course R175 forms a stable, bifurcated H-bond with Y120 and R114. These residues, in turn, stabilize the conformation of Y173 for productive binding via another direct H-bond (Figure 6a). All

Table 3. *In Vitro*/*in Silico* Site-Directed Mutagenesis of σ_1 Residues Belonging to the Region between the Protein SBDLI and SBDLII Motifs[a]

σ_1 residue	specific binding of PTZ (%)	ΔG_{bind} (kcal/mol)	$\Delta\Delta G_{bind}$[b] (kcal/mol)
wt	100	−10.02 (0.05)	−
S125A	49 (1.5)	−8.57 (0.09)	−1.45
T127A	45 (2.3)	−8.78 (0.11)	−1.24
V145A	78 (14)	−9.89 (0.07)	−0.13
F146A	57 (0.3)	−9.42 (0.09)	−0.60
Y147A	121 (4.1)	−8.80 (0.06)	−1.22
R175A	10 (4.1)	−8.00 (0.10)	−2.02

[a]Specific PTZ binding of different alanine mutants of the human σ_1 receptor and *in silico*-estimated free energy of binding (ΔG_{bind}) of the same σ_1 alanine mutants as generated by computational mutagenesis. Errors are given in parentheses as standard errors of the mean. [b]$\Delta\Delta G_{bind} = \Delta G_{bind,wt} - \Delta G_{bind,mutant}$.

dx.doi.org/10.1021/bi401575g | *Biochemistry* 2014, 53, 2993−3003

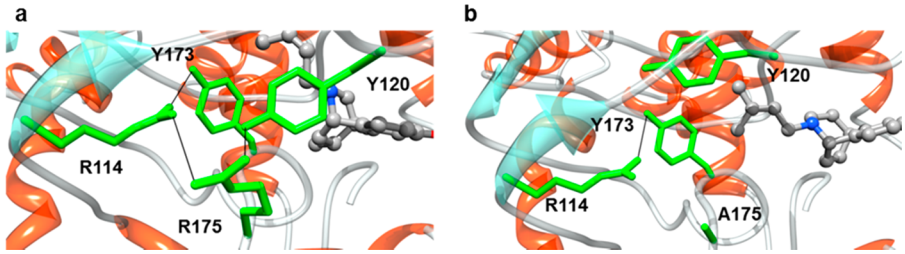

Figure 6. Details of the residues involved in a structurally stabilizing interaction of the (a) wt and (b) R175A mutant σ_1 receptor in complex with PTZ as obtained from equilibrated MD simulation snapshots. The protein backbone is shown as a transparent ribbon colored by secondary type (orange, α-helices; cyan, β-sheets; light gray, coils). The main residues involved in the interactions are shown as labeled green sticks. PTZ is shown as balls and sticks colored by element (C, gray; O, red; N, blue). In all panels, hydrogen atoms, water molecules, ions, and counterions were omitted for the sake of clarity.

these interactions translate into a −2.72 kcal/mol global favorable enthalpic contribution of these four amino acids to ligand binding, as detailed in Table 4. As discussed above, both

Table 4. Per Residue Free Energy Decomposition for wt and R175A Mutant σ_1 Receptors in Complex with PTZ[a]

wt	Y120	Y173	R175
R114	0.02	−0.91	−0.88
Y120	*	−0.26	−0.71
Y173	*	*	0.02
R175	*	*	*
$\sum\Delta H_{bind}$			**−2.72**
R175A	Y120	Y173	A175
R114	−0.01	−0.73	0.02
Y120	*	−0.03	−0.12
Y173	*	*	−0.02
A175	*	*	*
$\sum\Delta H_{bind}$			**−0.89**

[a]All energy values are in kilocalories per mole. Standard deviations range from ±0.01 to ±0.10.

Y120 and Y173 play a major role not only in direct PTZ binding but also in shaping the entire σ_1 binding site. Thus, replacing R175 with alanine results in an almost complete loss of the H-bond interaction network (Figure 6b): the aromatic interaction between Y120 and PTZ is lost, the entire binding site is enlarged, and the corresponding complex stabilization energy decreases dramatically [−0.89 kcal/mol (Table 4)].

CONCLUSIONS

The combined *in vitro*/*in silico* mutagenesis study reported here confirms some previous knowledge of the structural features of the σ_1 receptor and its binding site but also, and perhaps more importantly, qualifies and quantifies the role of several receptor residues that figure prominently in receptor−ligand binding. Specifically, among those residues belonging to the putative receptor binding pocket, replacing I128 and Y173 with alanine almost abrogates PTZ binding, which is consistent with a drastic reduction of stabilizing, hydrophobic interactions. The specific nature of the anionic residue E172 is critical for PTZ binding in that not only its replacement with alanine but also an exchange with a residue of a similar nature but with a smaller side chain (E172D) results in the total failure of receptor ligand binding. The role of σ_1 amino acids belonging to the SBDLI and -II domains has been differentiated and rationalized: while a critical role in maintaining the protein secondary structure of this protein portion with respect to the cellular membrane has been verified for those residues belonging to the first domain, mutagenesis performed on residues in the SDBLII region did not affect the affinity of the receptor for PTZ. The removal of small sequences from the C-terminal part of the protein (e.g., seven residues) resulted in a substantial decrease in ligand binding activity, as these deletions result in a general reconfiguration of the receptor binding pocket, ultimately involving those residues that constitute the PTZ main anchor points. Finally, this combined approach unveiled the substantial role exerted by other σ_1 residues in ligand binding; for instance, the series of polar residues S125, T127, and R175 all serve to maintain the high affinity of the σ_1 receptor for PTZ, and their replacement with the small, apolar alanine results in a neat decrease in receptor ligand binding activity.

ASSOCIATED CONTENT

Supporting Information

Materials, Figures S1−S4, Tables S1−S4, computational details, and references. This material is available free of charge via the Internet at http://pubs.acs.org.

AUTHOR INFORMATION

Corresponding Authors

*E-mail: wuensch@uni-muenster.de. Phone: +39 040 558 3750.
*E-mail: sabrina.pricl@di3.units.it.

Author Contributions

S.B. and E.L. contributed equally to this work.

Funding

This work was supported by the Deutsche Forschungsgemeinschaft, which is gratefully acknowledged. Access to CINECA supercomputers Eurora and Fermi (Bologna, Italy) was granted via MONALISA, NANO4HEALTH, and INSIDER projects (Iscra supercomputing grants to E.L. and S.P.).

Notes

The authors declare no competing financial interest.

REFERENCES

(1) Matsumoto, R. R., Liu, Y., Lerner, M., Howard, E. W., and Brackett, D. J. (2003) Sigma receptors: Potential medications development target for anti-cocaine agents. *Eur. J. Pharmacol. 469*, 1−12.
(2) Gilbert, P. E., and Martin, W. R. (1976) The effects of morphine and nalorphine-like drugs in the nondependent and morphine-dependent chronic spinal dog. *J. Pharmacol. Exp. Ther. 197*, 517−532.
(3) Gundlach, A. L., Largent, B. L., and Snyder, S. H. (1985) Phencyclidine and sigma opiate receptors in brain: Biochemical and autoradiographical differentiation. *Eur. J. Pharmacol. 113*, 465−466.
(4) Hayashi, T., and Su, T. P. (2004) Sigma-1 receptor ligands: Potential in the treatment of neuropsychiatric disorders. *CNS Drugs 18*, 269−284.

(5) Fontanilla, D., et al. (2009) The Hallucinogen N,N-Dimethyltryptamine (DMT) Is an Endogenous Sigma-1 Receptor Regulator. *Science 323*, 934−937.
(6) Hanner, M., et al. (1996) Purification, molecular cloning, and expression of the mammalian sigma1-binding site. *Proc. Natl. Acad. Sci. U.S.A. 93*, 8072−8077.
(7) Kekuda, R., Prasad, P. D., Fei, Y. J., Leibach, F. H., and Ganapathy, V. (1996) Cloning and functional expression of the human type 1 sigma receptor (hSigmaR1). *Biochem. Biophys. Res. Commun. 229*, 553−558.
(8) Maurice, T., and Su, T. P. (2009) The pharmacology of sigma-1 receptors. *Pharmacol. Ther. 124*, 195−206.
(9) Cobos, E. J., Entrena, J. M., Nieto, F. R., Cendan, C. M., and DelPezo, E. (2008) Pharmacology and therapeutic potential of sigma1 receptor ligands. *Curr. Pharmacol. 6*, 344−366.
(10) Ishikawa, M., and Hashimoto, K. (2010) The role of sigma-1 receptors in the pathophysiology of neuropsychiatric diseases. *J. Recept., Ligand Channel Res. 3*, 25−36.
(11) Collina, S., et al. (2013) Sigma receptor modulators: A patent review. *Expert Opin. Ther. Pat. 23*, 597−613.
(12) Choi, S. R., et al. (2001) Development of a Tc-99m labeled sigma-2 receptor-specific ligand as a potential breast tumor imaging agent. *Nucl. Med. Biol. 28*, 657−666.
(13) Tu, Z., et al. (2007) Fluorine-18-labeled benzamide analogues for imaging the σ2 receptor status of solid tumors with positron emission tomography. *J. Med. Chem. 50*, 3194−3204.
(14) Bowen, W. D. (1993) [^{3}H]-(+)-Pentazocine: A potent and highly selective benzomorphan-based probe for sigma-1 receptors. *Mol. Neuropharmacol. 3*, 117−126.
(15) Okuyama, S., and Nakazato, A. (1996) NE-100: A novel sigma receptor antagonist. *CNS Drug Rev. 2*, 226−237.
(16) McCann, D. J., and Su, T. P. (1990) Haloperidol-sensitive (+)[^{3}H]SKF-10,047 binding sites (σ sites) exhibit a unique distribution in rat brain subcellular fractions. *Eur. J. Pharmacol., Mol. Pharmacol. Sect. 188*, 211−218.
(17) Aydar, E., Palmer, C. P., Klyachko, V. A., and Jackson, M. B. (2002) The sigma receptor as a ligand-regulated auxiliary potassium channel subunit. *Neuron 34*, 399−410.
(18) Russ, W. P., and Engelman, D. M. (2000) The GXXXG motif: A framework for transmembrane helix-helix association. *J. Mol. Biol. 296*, 911−919.
(19) Seth, P., et al. (2001) Expression pattern of the type 1 sigma receptor in the brain and identity of critical anionic amino acid residues in the ligand-binding domain of the receptor. *Biochim. Biophys. Acta 1540*, 59−67.
(20) Kahoun, J. R., and Ruoho, A. E. (1992) (^{125}I)iodoazidococaine, a photoaffinity label for the haloperidol-sensitive sigma receptor. *Proc. Natl. Acad. Sci. U.S.A. 89*, 1393−1397.
(21) Laurini, E., et al. (2011) Homology model and docking-based virtual screening for ligands of the σ1 receptor. *ACS Med. Chem. Lett. 2*, 834−839.
(22) Laurini, E., et al. (2012) Another brick in the wall. Validation of the σ1 receptor 3D model by computer-assisted design, synthesis, and activity of new σ1 ligands. *Mol. Pharmaceutics 9*, 3107−3126.
(23) Yamamoto, H., et al. (1999) Amino acid residues in the transmembrane domain of the type 1 sigma receptor critical for ligand binding. *FEBS Lett. 445*, 19−22.
(24) Palmer, C. P., Mahen, R., Schnell, E., Djamgoz, M. B. A., and Aydar, E. (2007) Sigma-1 receptors bind cholesterol and remodel lipid rafts in breast cancer cell lines. *Cancer Res. 67*, 11166−11175.
(25) Pal, A., et al. (2008) Juxtaposition of the steroid binding domain-like I and II regions constitutes a ligand binding site in the α-1 receptor. *J. Biol. Chem. 283*, 19646−19656.
(26) Lowry, O. H., Rosebrough, N. J., Farr, A. L., and Randall, R. J. (1951) Protein measurement with the Folin phenol reagent. *J. Biol. Chem. 193*, 265−275.
(27) Woolf, T. B., and Roux, B. (1996) Structure, energetics, and dynamics of lipid-protein interactions: A molecular dynamics study of the gramicidin A channel in a DMPC bilayer. *Proteins 24*, 92−114.
(28) Jo, S., Kim, T., and Im, W. (2007) Automated builder and database of protein/membrane complexes for molecular dynamics simulations. *PLoS One 2*, e880.
(29) Jorgensen, W. L., Chandrasekhar, J., Madura, J. D., Impey, R. W., and Klein, M. L. (1983) Comparison of simple potential functions for simulating liquid water. *J. Chem. Phys. 79*, 926−935.
(30) Skjevik, Å. A., Madej, B. D., Walker, R. C., and Teigen, K. (2012) LIPID11: A modular framework for lipid simulations using Amber. *J. Phys. Chem. B 116*, 11124−11136.
(31) Duan, Y., et al. (2003) Point-charge force field for molecular mechanics simulations of proteins based on condensed-phase quantum mechanical calculations. *J. Comput. Chem. 24*, 1999−2012.
(32) Meyer, C., et al. (2012) Pd-catalyzed direct C-H bond functionalization of spirocyclic σ(1) ligands: Generation of a pharmacophore model and analysis of the reverse binding mode by docking into a 3D homology model of the σ_1 receptor. *J. Med. Chem. 55*, 8047−8065.
(33) Laurini, E., Dal Col, V., Wünsch, B., and Pricl, S. (2013) Analysis of the molecular interactions of the potent analgesic S1RA with the σ1 receptor. *Bioorg. Med. Chem. Lett. 23*, 2868−2871.
(34) Rossi, D., et al. (2013) Chemical, Pharmacological, and in vitro Metabolic Stability Studies on Enantiomerically Pure RC-33 Compounds: Promising Neuroprotective Agents Acting as σ1 Receptor Agonists. *ChemMedChem 8*, 1514−1527.
(35) Case, D.-A., et al. (2012) *Amber 12*, University of California, San Francisco.
(36) Ryckaert, J. P., Ciccotti, G., and Berendsen, H. J. C. (1977) Numerical integration of the cartesian equations of motion of a system with constraints: Molecular dynamics of n-alkanes. *J. Comput. Phys. 23*, 327−341.
(37) Srinivasan, J., Cheatham, T. E., III, Cieplak, P., Kollman, P. A., and Case, D. A. (1998) Continuum solvent studies of the stability of DNA, RNA and phosphoramidate-DNA helices. *J. Am. Chem. Soc. 120*, 9401−9409.
(38) Laurini, E., et al. (2013) Through the open door: Preferential binding of dasatinib to the active form of BCR-ABL unveiled by in silico experiments. *Mol. Oncol. 7*, 968−975.
(39) Onufriev, A., Bashford, D., and Case, D. A. (2000) Modification of the generalized Born model suitable for macromolecules. *J. Phys. Chem. B 104*, 3712−3720.
(40) Feig, M., et al. (2004) Performance comparison of generalized Born and Poisson methods in the calculation of electrostatic solvation energies for protein structures. *J. Comput. Chem. 25*, 265−284.
(41) http://www.esteco.com/home/mode_frontier/mode_frontier.html.
(42) Chu, U. M., Ramachandran, S., Hajipour, A. R., and Ruoho, A. E. (2013) Photoaffinity Labeling of the Sigma-1 Receptor with N-[3-(4-Nitrophenyl)propyl]-N-dodecylamine: Evidence of Receptor Dimers. *Biochemistry 52*, 859−868.